Perfusion Quantification of Liver Metastases of Colorectal Cancer Treated with Anti-angiogenic-Based Therapy: Assessment of Intra- and Inter-observer Reproducibility of Parameters in Three Regions of Interest Outlining Lesions

Paul-Armand Dujardin, Julie Léger, Thierry Lecomte, Frédéric Patat, Guillaume Chassagnon, Aurore Bleuzen

Title: Perfusion quantification of liver metastases of colorectal cancer treated with antiangiogenic-based therapy: assessment of intra- and inter-observer reproducibility of parameters in three regions of interest outlining lesions.

Authors: Paul-Armand Dujardin[1], Julie Léger[1], Thierry Lecomte[2,3], Frédéric Patat[1,4], Guillaume Chassagnon[1,4], Aurore Bleuzen[1,4]

[1]: CIC 1415, CHU Tours, Inserm, Tours Cedex, France

[2]: Department of Hepato-gastroenterology and Digestive Oncology, CHRU Tours, 37044, Tours Cedex, France

[3]: EA 7501 GICC, Tours University, Tours, France

[4]: Groupement d'Imagerie Médicale, CHRU Tours, 37044, Tours Cedex, France

Corresponding author:

Paul-Armand Dujardin

CIC 1415, CHU Tours, Inserm, Tours Cedex, France

Phone: (+33) 247479791

Fax: (+33) 247473876

E-mail: paul-armand.dujardin@chu-tours.fr

Abstract

This study evaluates the reproducibility of dynamic contrast-enhanced ultrasound (DCEUS) parameters outlining liver metastases of colorectal cancer in 45 patients, pre- and post-antiangiogenic-based therapy. Tumor enhancement was quantified by drawing three regions of interest (ROI): 1 outlining the tumor based on portal phase DCEUS images, 1 in the hypoenhanced center of the lesion and 1 outlining the lesion using parametric imaging. Perfusion parameters were extracted from time-intensity curves. Another ROI was drawn in healthy liver parenchyma for normalization. Intra- and inter-observer reproducibility of these parameters was evaluated using intraclass correlation coefficients (ICC). For the 3 ROIs, both intra- and inter-observer reproducibility were excellent (ICC≥0.9) for 50.8% absolute parameters and were moderate to good (0.7≤ICC<0.9) for 26.7% of them. In healthy liver parenchyma and for normalized parameters, reproducibility was moderate to excellent for 59.4% of intensity parameters and was low (ICC<0.7) for almost all temporal parameters. This study demonstrates that DCEUS is a reproducible tool for evaluating perfusion parameters.

Key-words: Reproducibility, Colorectal cancer, Ultrasound, Quantification, Liver metastases

Introduction

In recent years, a lot of studies focused on the evaluation of tumor response by functional imaging, making this technique getting a growing role in oncology (Goh et al. 2007). Indeed, targeted therapies such as angiogenesis inhibitors have cytostatic effects that lead to more complex changes than classical cytotoxic chemotherapy. Thus, necrosis and cavitation without a decrease of the volume are frequently observed (Desar et al. 2009), making RECIST (Response Evaluation Criteria In Solid Tumors) (Eisenhauer et al. 2009) sometimes insufficient to estimate anti-tumor efficacy of antiangiogenic therapies (Choi et al. 2007; Chun et al. 2009; Grothey and Allegra 2012; Krajewski et al. 2011; Shindoh et al. 2012).

The use of bevacizumab (Avastin, Genentech Inc., South San Francisco, California), an anti-VEGF antibody, is associated with a significant increase in progression-free survival of patients with metastatic colorectal cancer (Hurwitz et al. 2004). Since its introduction and approval, several imaging techniques have been explored to improve the assessment of its therapeutic efficacy including quantitative imaging (Coenegrachts et al. 2012; De Bruyne et al. 2012; Morgan et al. 2003; Schirin-Sokhan et al. 2012; Tranquart et al. 2017; Wu et al. 2017). Among these techniques, quantitative dynamic contrast-enhanced ultrasonography (DCEUS) has already demonstrated its ability to improve the follow-up of various types of tumors treated with antiangiogenic agents by predicting the efficacy or the lack of efficacy of such antiangiogenic therapies (Lassau et al. 2006; Lassau et al. 2010; Lassau et al. 2011; Lassau et al. 2014; Schirin-Sokhan et al. 2012; Tranquart et al. 2017; Wu et al. 2017).

Quantitative DCEUS relies on the analysis of perfusion parameters extracted from time-intensity curves representing perfusion kinetics of different regions of analysis, generally the lesion and a reference tissue (Tranquart et al. 2012). Although European Federation of Societies for Ultrasound in Medicine and Biology (EFSUMB) recently edited

recommendations for the acquisition of quantitative DCEUS (Dietrich et al. 2012) and guidelines for contrast-enhanced ultrasound (CEUS) (Claudon et al. 2013; Dietrich et al. 2018), no study have either evaluated the reproducibility of quantified DCEUS, or clearly specified how the lesions were delineated.

The goal of this study was to evaluate reproducibility of perfusion parameters extracted from the quantification of perfusion of colorectal cancer liver metastases, before administration of bevacizumab and for assessment of the evolution of metastases' perfusion 15 days after treatment. For this purpose, liver metastases were delineated with 3 different regions of interest, from the hypoenhanced center of the lesion to the peripheral enhanced rim.

Materials and methods:

Patients

Patients were included among the 137 included in a multicenter, prospective, interventional cohort study designed to evaluate the usefulness of quantitative DCEUS for early evaluation of tumor response to bevacizumab in metastatic colorectal cancer (NCT00489697) (Tranquart et al. 2017). First, patients with available DCEUS exams at both D0 and D15, and whose exam quality was sufficient to perform correct quantification (meaning for example no technical problem or lesion's motion within the scanning plane allowing correct motion compensation) were selected. Then, the website www.random.org was used to randomly select half of the remaining patients finally included in this study. Local ethics committee approved the study and patients gave their written informed consent prior to their inclusion. From January 2007 to December 2012, patients with previously untreated and unresectable histologically confirmed metastatic colorectal cancer (CRC) were included and followed for 2 years in 9 French university hospitals. Patients received bevacizumab-based chemotherapy until disease progression or unacceptable toxicity occurred. Liver metastases had to be larger than 5 mm without exceeding 50 mm. Exclusion criteria included any contraindication to Bevacizumab or to Sonovue® (Bracco, Milan, Italia), a prior chemotherapy for metastatic CRC, a surgery within 28 days of starting bevacizumab, a history of malignancy other than metastatic CRC and pregnancy. Bevacizumab was prescribed as complement of conventional chemotherapy, chosen at the clinician's discretion.

DCEUS

DCEUS exams were performed in each institution by physicians with 2 to 9 years' experience in practice of contrast-enhanced ultrasonography. For each patient, 5 examinations were performed according to the protocol. Among these examinations, 2 were selected for this

study: one within 8 days before the first injection of Bevacizumab (D0) and in the 24 hours preceding the second infusion of bevacizumab on day 15 (D15). Those 2 time points were chosen in order to evaluate the reproducibility of DCEUS quantification at baseline and after a delay that was previously published as sufficient to observe efficiency or non-efficiency of bevacizumab-based chemotherapy (Schirin-Sokhan et al. 2012; Tranquart et al. 2017). All selected patients had DCEUS performed on Sequoia™ 512 scanners (Siemens, Mountain View, CA, USA) with a 1-4.5 MHz 4C1 curved array transducer using Cadence Contrast Pulse Sequencing (CPS) imaging mode.

Conventional B-mode sonography was performed to identify the target lesion. To assess perfusion of the target lesion, a bolus intravenous injection of 2.4mL of Sonovue® followed by a flush of 10mL of saline was performed using a needle catheter of at least 20G. Cine-loops of 80 seconds were recorded at the level of the target lesion.

Image analysis

Image analysis was performed with dedicated software VueBox™ (Bracco Suisse SA, Plan-les-Ouates, Switzerland). Enhancement can be determined by calculating relative echopower values in a region of interest (ROI). A mathematical model allows a curve fitting of the time intensity curve (TIC) leading to generating 10 parameters based on indicator-dilution theory: 4 related to blood volume (peak enhancement (PE, the maximum intensity), area under the curve during wash-in (WiAUC), area under the curve during wash-out (WoAUC), total area under the curve (AUC = WiAUC + WoAUC)), 5 related to blood flow (time to peak (TTP, the time between the beginning of the clip and the time to peak intensity), rise time (RT, wash-in time), fall time (FT, wash-out time), wash-in rate (WiR, the maximum slope during the wash-in) and wash-out rate (WoR, the maximum slope during the wash-out))

and mean transit time (mTT) (Tranquart et al. 2012). The quality of the mathematical fit was also extracted.

The enhancement was evaluated within 4 ROIs (Fig. 1). A first ROI was drawn in normal liver parenchyma at a similar depth if possible of the lesion and serving as a reference (Tranquart et al. 2012). Then, 3 ROIs (ROI-1 to 3) were drawn in the target lesion. ROI-1 and -2 were drawn based on DCEUS images during portal phase with ROI-1 outlining the lesion (Fig 1a) and ROI-2 placed in its hypoenhanced center (Fig 1b). The drawing of ROI-3 was realized from a parametric image of WiAUC parameter (Fig 1c), outlining the lesion. WiAUC's parametric imaging is a color representation where each pixel of the analyzed region is colored according to its WiAUC value. If the entire drawing of ROI-3 was not possible on the parametric image, then DCEUS images were used to delineate the rest of the lesion. ROIs drawings were performed by 2 independent operators according to the same guidelines in order to evaluate inter-observer reproducibility. Measurements were repeated once by the first operator 2 weeks after the 1st quantifications had been realized in order to assess intra-observer reproducibility. Quantifications were done under the supervision of a physician experienced in practice of contrast-enhanced ultrasonography.

Ten parameters were obtained for each ROI at D0 and D15. Absolute values and values relative to the healthy liver (in percent, determined by the ratio lesion/reference*100) were considered for ROI-1 to ROI-3. The reproducibility of perfusion parameters was assessed at D0 and for the evolution of the parameters as follows: D15-D0 =100*(D15-D0)/D0. Areas of ROI-1 to -3 were also measured. Lastly, during each quantification, the 2 operators rated quality of parametric imaging according to a 4-level scale (≥75%, 50 to 74%, 10 to 49% and <10%), based on the percentage of the contours of the lesion that could be delineated on WiAUC's parametric imaging. Quality of parametric imaging was rated to test its ability to correctly delineate the lesions.

Statistical analysis

Patients were described using median and interquartile range (IQR, [Q1 ; Q3]) for quantitative data and using frequencies and percent for qualitative data. Intra- and inter-observer reproducibility was assessed by estimating intraclass correlation coefficients (ICCs) and their 95% confidence interval (95% CI). Then, we evaluated 2 ways for assessing reproducibility of 10 parameters (6 intensity parameters and 4 temporal parameters) in 3 ROIs for each lesion, at D0 and D15, resulting in 120 analyses for the lesions for absolute parameters and 120 for normalized parameters.

Quality of parametric imaging (≥75%, 50 to 74%, 10 to 49% and <10%) was described with frequencies and percent, and areas of the three ROIs and quality of the mathematical fit were described using median and IQR and were compared using Friedman test. First, a global comparison was performed and then pairwise comparisons were done to identify which ROI was different in terms of area or quality of fit. Analyses were performed by considering the mean of the 2 measures (area and quality of fit) of the 2 observers. Statistical analyses were performed using statistical analysis software (SAS 9.3, SAS institute, Cary, NC) and R 3.3.1 (R Development Core Team 2016). A p-value of 0.05 was considered as significant.

Results

Among the 137 patients available, 26 patients did not have both D0 and D15 exam (technical problem, death prior to D15 or premature end of study) and 20 did not have sufficient quality to perform quantification. Of the remaining 91 patients, 45 were randomly selected in this study.

The patient characteristics are described in Tab. 1. The median age of patients was 64 years (IQR [59; 71]) with 66.7% being males. Primary tumor was colic in 73.3% of cases. No difficulty was encountered during quantification.

Reproducibility of absolute parameters in ROIs outlining the lesion (Tab. 2, Fig. 2).

At D0, a large majority of parameters (42/60, 70%) showed an excellent intra- and inter-observer reproducibility (ICC $\geq$ 0.9) in the 3 ROIs. Moreover, intensity parameters (PE, WiAUC, WiR, WoAUC, AUC and WoR) showed a better reproducibility, with ICC values superior to 0.9, than temporal parameters (RT, mTT, TTP, FT).

For the evolution D15-D0, all intensity parameters showed excellent intra-observer reproducibility in the 3 ROIs. On the opposite, temporal parameters did not show such a good reproducibility, but remained at least moderate (0.7 $\leq$ ICC < 0.8), except for mTT where reproducibility was poor. Inter-observer reproducibility was similar for temporal parameters but decreased for intensity parameters.

Globally, the overall reproducibility of absolute parameters was similar between the 3 ROIs. The only observable difference stands in inter-observer reproducibility for the evolution D15-D0: the reproducibility was slightly better for ROI-1 (delineation of the tumor based on portal phase DCEUS images) than for ROI-3 (delineation based on WiAUC's parametric imaging) and was low for ROI-2 (ROI in the hypoenhanced center of the lesion).

Besides, intra-observer reproducibility was better than inter-observer reproducibility, especially for the evolution D15-D0 and for temporal parameters at D0.

Reproducibility of parameters in healthy liver parenchyma (Tab. 3, Fig. 2)

At D0 and for the evolution D15-D0, intensity parameters in healthy liver parenchyma showed a moderate to excellent intra- and inter-observer reproducibility. Concerning temporal parameters, only TTP showed at least moderate reproducibility.

Besides, intra-observer reproducibility was lower than inter-observer reproducibility at D0, but was better for the evolution D15-D0.

Reproducibility of normalized parameters in ROIs outlining the lesion (Tab. 4, Fig. 2).

At D0, a large majority of intensity parameters (29/36, 80.6%) showed a least a moderate intra- and inter-observer reproducibility in the 3 ROIs. For the evolution D15-D0, only a third of intensity parameters (6/18, 33.3%) showed at least a moderate intra-observer reproducibility in the 3 ROIs. Only WiR showed moderate inter-observer reproducibility in the 3 ROIs.

For temporal parameters, almost none of them (2/36, 5.6%) showed at least moderate intra- or inter-observer reproducibility in the 3 ROIs, either at D0 or for the evolution D15-D0.

Globally, the overall reproducibility of normalized parameters was similar between the 3 ROIs. Besides, intra- and inter-observer reproducibilities were also similar.

Quality of WiAUC's parametric imaging (Tab. 5)

85.2% of the lesions were assessed as well defined (quality ≥ 50%) and 58.5% were assessed as very well defined (quality ≥ 75%). Only 4.8% of the lesions were assessed as badly defined (quality < 10%) on WiAUC's parametric imaging.

Area of the ROIs (Tab. 5)

Areas of the 3 ROIs were significantly different at D0 and D15 ($p < 0.0001$).

With pairwise analysis, ROI-2 was smaller than ROI-1 at D0 and D15 (3.3 cm² [1.4 ; 6.2] vs 6.2 cm² [3.5 ; 12.7], $p < 0.0001$ and 2.6 cm² [1.2 ; 5.3] vs 5.2cm² [2.9 ; 11.1], $p < 0.0001$ respectively) and ROI-3 (3.3 cm² [1.4 ; 6.2] vs 7.1 cm² [4.0 ; 13.5], $p < 0.0001$ and 2.6 cm² [1.2 ; 5.3] vs 6.1 cm² [3.7 ; 10.9], $p < 0.0001$ respectively).

ROI-1 was also smaller than ROI-3 at D0 and D15 (6.2 cm² [3.5 ; 12.7] vs 7.1 cm² [4.0 ; 13.5], $p < 0.0001$ and 5.2 cm² [2.9 ; 11.1] vs 6.1cm² [3.7 ; 10.9], $p < 0.0001$ respectively).

Quality of the mathematical fit (Tab. 5)

Quality of fit of the 3 ROIs were significantly different at D0 and D15 ($p = 0.0004$ and $p = 0.022$ respectively).

With pairwise analysis, at D0, ROI-2 had a lower quality of fit than ROI-1 (89.8% [74.8 ; 97.0] vs 92.3% [80.6 ; 96.7], $p = 0.0017$) and ROI-3 (89.8% [74.8 ; 97.0] vs 93.1% [87.6 ; 96.4], $p = 0.0017$). Quality of fit of ROI-1 and ROI-3 were not significantly different at D0.

At D15, only ROI-2 had a lower quality of fit than ROI-1 (86.9% [76.8 ; 94.7] vs 89.4% [82.7 ; 95.7], $p = 0.0046$).

Discussion

Microvascularization of liver metastases of colorectal tumors is known to be heterogeneous (Konerding et al. 2001). As a result, imaging of microvascularization is also heterogeneous, and there should be a standard for perfusion quantification. In the present study, we have shown that quantitative DCEUS allows reproducible assessment of perfusion parameters of liver metastasis from colorectal cancer treated by bevacizumab, and thus for 3 different means of delineating a lesion (based on DCEUS portal phase or WiAUC's parametric imaging). In previous studies, PE, AUC, TTP and RT are the main parameters associated to liver metastases' response to antiangiogenic therapy (Lassau et al. 2014; Schirin-Sokhan et al. 2012; Tranquart et al. 2017; Wu et al. 2017). These parameters showed moderate to excellent reproducibility, confirming their potential to help clinicians identifying patients responding to therapy (Gauthier et al. 2011). However, one study had evaluated mTT as a predictive parameter to identify patients with increased freedom from progression (Lassau et al. 2016), but this parameter showed the poorest reproducibility in our study.

We found only one study that has evaluated reproducibility of parameters depending on the drawing of regions of interest (Atri et al. 2016). They positioned 2 ROIs: one outlining the lesion in B-mode images and one outlining the highest enhanced signal on DCEUS images, avoiding necrosis. The positioning of the lesion was different to ours; nevertheless, the ROI positioned based to B-mode images may be close to our ROI outlining the lesion based on portal phase DCEUS images (ROI-1). They found a strong inter-observer reproducibility of a parameter related to blood volume (with disruption-replenishment technique). This is coherent with our results, as the absolute intensity parameters showed an excellent inter-observer reproducibility.

In most of previously published studies, rules used to draw ROIs have not been precisely described; although, we supposed that most of studies used a ROI like ROI-1, that

being a ROI outlining tumors using portal phase DCEUS images, to delineate the lesions. Indeed, portal phase is the time where the contrast between liver metastases and healthy liver parenchyma is the highest. To overcome this limitation, we aimed to evaluate whether parametric imaging could help drawing more precise and accurate ROIs. We observed a good delineation of the lesion in 85.2% of the cases and a good quality of the mathematical fit with WiAUC‘s parametric imaging, indicating the technical feasibility of this technique. ROIs delineated on parametric imaging were significantly larger than those delineating the tumor on portal phase, allowing them to include a part of the peripheral hyperenhanced rim. Indeed, in our experience, we noticed that the hypoenhanced lacuna used to define the lesion on portal or late phase (Claudon et al. 2013) often excludes a large part of the hyperenhanced rim seen on the arterial phase (Fig. 3) (Dietrich et al. 2018; Lyshchik et al. 2018) which corresponds to areas of high microvascular density and neoangiogenesis (Konerding et al. 2001). Thus, the use of WiAUC’s parametric imaging could be a good alternative, especially since the corresponding ROI (ROI-3) presented similar reproducibility than ROIs delineating lesions on portal phase DCEUS images (ROI-1); only inter-observer reproducibility of absolute parameters for the evolution D15-D0 was slightly lower. This may be related to the variability of thresholding WiAUC’s parametric imaging using a color look-up table. Indeed, thresholding was obtained from the distribution of WiAUC’s value of pixels in the reference ROI drawn in healthy liver parenchyma, which showed at best a good reproducibility (ICC < 0.9).

Lower inter-observer reproducibility of parameters in ROI-2 is consistent with the results of Goh *et al.* who demonstrated that smaller ROIs had higher variability in the assessment of the perfusion of primary colorectal tumors by perfusion CT (Goh et al. 2008). Indeed, ROI-2, placed in tumors hypoenhanced center, were significantly smaller than the two other ROIs. This lower inter-observer reproducibility may also be related to the several

possible ways to draw a ROI in the center of the lesions. Besides, we showed that the quality of the mathematical fit for evaluating perfusion parameters was the lowest in ROI-2, making this ROI less attractive to correctly evaluate tumor perfusion.

The majority of previous studies had only assessed the absolute values of perfusion parameters (Lassau et al. 2006; Lassau et al. 2011; Lassau et al. 2014; Williams et al. 2011), but it is now possible to normalize them by using a reference tissue corresponding to healthy liver parenchyma (Tranquart et al. 2012). Reference tissue is used as arterial input function and allows assessment of relative values of intensity-related parameters, by taking into account the effects of bolus injection and ultrasound attenuation. Indeed, signal intensity is known to vary from a bolus injection to another, even during the same examination (Williams et al. 2011). Interestingly, our study showed that normalization is associated to a reduction of reproducibility, especially for temporal parameters. However, reproducibility of normalized intensity parameters remained moderate. This decrease is concordant with the lower reproducibility of parameters estimated in healthy liver parenchyma, mainly due to the heterogeneity of liver perfusion in DCEUS and to the multiple ways to draw a ROI within the liver, even when rules have been established. Our results are opposite to those of Payen *et al.* who found that normalization decreases variability in renal neuroblastoma of mice (Payen et al. 2011).

This study has some limitations mainly related to the empirical choices we made to define the rules used to draw the 3 ROIs, in the absence of any previous data in the literature to support such drawing. For delineation of ROI-3 on parametric imaging, we selected WiAUC's parametric imaging as it is a marker of an increased vascularity of a lesion and as it seemed appropriate for possibly include the hyperenhanced rim. Besides, AUC seems to be the best marker associated with response to therapy, freedom from progression and overall survival (Lassau et al. 2014; Tranquart et al. 2017). With VueBox^{TM}, thresholding of

parametric imaging is based on the distribution of values in the first ROI drawn after motion compensation. In our experience, thresholding obtained by using the ROI positioned in healthy liver parenchyma appeared to be the most reproducible, even if the reference ROI is positioned in a very different position. Another limitation of our study is that we only assessed reproducibility of the post-processing. Indeed, reproducibility of the whole chain from acquisition to quantification has not been evaluated in this study and should be lower than that we observed.

In conclusion, quantification of liver metastases of colorectal cancer to assess perfusion parameters is a reproducible technique. The reproducibility is equivalent whether delineating the lesion based on portal phase images or by using a parametric image taking into account the enhancement characteristics of the lesions. There is a decrease of the reproducibility of the perfusion parameters when they are normalized to those of healthy liver parenchyma because this latter is quite heterogeneous and positioning a region of interest inside it remains challenging.

Conclusions

In DCEUS, delineation of liver metastases of colorectal cancer based on portal phase or based on parametric imaging allows good reproducibility in order to assess perfusion quantification and its early evolution under treatment with bevacizumab. Delineation based on WiAUC's parametric imaging has the advantage to better take into account the hyperenhanced rim of the tumors, which reflects tumor angiogenesis. Normalization of perfusion parameters is associated to a decrease of reproducibility due to a lower reproducibility of the parameters quantified in healthy liver parenchyma, despite the use of previously reported guidelines. Nevertheless, the reproducibility remained acceptable for intensity parameters.

Table 1: Patient characteristics. Quantitative variables are described using quartiles, and qualitative variables are described using numbers and frequencies.

Variable	Values
Age (years)	64.0 [59.0 ; 71.0]
Gender	Male: 30 (66.7)
	Female: 15 (33.3)
Weight (kg)	65.0 [60.0, 76.0]
Height (cm)	170.0 [163.0, 175.0]
WHO status[1]	Normal: 21 (48.8)
	Reduced activity: 20 (46.5)
	Work not possible: 2 (4.7)
Localization of the primary tumor	Colon: 33 (73.3)
	Rectum: 12 (26.7)

[1] total = 43

Table 2: ICC values and their 95% confidence interval for evaluating reproducibility of absolute perfusion parameters.

ICC = intraclass correlation coefficient

Inter = Inter-observer reproducibility

Intra = intra-observer reproducibility

ROI-1: drawing outlining the lesion in the portal phase DCEUS images

ROI-2: drawing positioned in the hypoenhanced center of the lesion

ROI-3: drawing outlining the lesion based on WiAUC's parametric imaging

	Day 0		Evolution from day 0 to day 15	
Perfusion parameter	Intra	Inter	Intra	Inter
PE				
ROI-1	**0.980 [0.963 ; 0.989]**	**0.969 [0.944 ; 0.983]**	**0.967 [0.940 ; 0.982]**	**0.779 [0.633 ; 0.872]**
ROI-2	**0.956 [0.921 ; 0.975]**	**0.956 [0.922 ; 0.976]**	**0.951 [0.914 ; 0.973]**	**0.292 [0.004 ; 0.537]**
ROI-3	**0.960 [0.928 ; 0.978]**	**0.975 [0.955 ; 0.986]**	**0.988 [0.978 ; 0.993]**	**0.661 [0.460 ; 0.798]**
WiAUC				
ROI-1	**0.972 [0.949 ; 0.984]**	**0.983 [0.970 ; 0.991]**	**0.969 [0.945 ; 0.983]**	**0.850 [0.744 ; 0.915]**
ROI-2	**0.956 [0.922 ; 0.976]**	**0.963 [0.933 ; 0.979]**	**0.966 [0.939 ; 0.981]**	**0.707 [0.526 ; 0.827]**
ROI-3	**0.934 [0.884 ; 0.963]**	**0.904 [0.833 ; 0.946]**	**0.966 [0.939 ; 0.981]**	**0.772 [0.622 ; 0.868]**
RT				
ROI-1	0.966 [0.939 ; 0.981]	0.622 [0.407 ; 0.773]	0.796 [0.659 ; 0.882]	0.843 [0.733 ; 0.910]
ROI-2	0.827 [0.707 ; 0.901]	0.517 [0.269 ; 0.702]	0.826 [0.706 ; 0.901]	0.795 [0.657 ; 0.881]
ROI-3	0.966 [0.939 ; 0.981]	0.637 [0.427 ; 0.782]	0.838 [0.725 ; 0.908]	0.778 [0.632 ; 0.872]
mTT				
ROI-1	0.686 [0.495 ; 0.814]	0.361 [0.081 ; 0.589]	0.468 [0.208 ; 0.667]	0.240 [0.000 ; 0.495]
ROI-2	0.317 [0.031 ; 0.555]	0.162 [0.000 ; 0.431]	0.480 [0.222 ; 0.675]	0.327 [0.042 ; 0.563]
ROI-3	0.311 [0.025 ; 0.551]	0.322 [0.037 ; 0.559]	0.528 [0.283 ; 0.709]	0.533 [0.289 ; 0.713]
TTP				

ROI-1	0.957 [0.924 ; 0.976]	0.874 [0.783 ; 0.929]	0.877 [0.787 ; 0.930]	0.866 [0.770 ; 0.924]
ROI-2	0.822 [0.699 ; 0.898]	0.804 [0.672 ; 0.887]	0.852 [0.747 ; 0.916]	0.852 [0.747 ; 0.916]
ROI-3	0.965 [0.938 ; 0.981]	0.880 [0.792 ; 0.932]	0.906 [0.835 ; 0.947]	0.831 [0.714 ; 0.903]
WiR				
ROI-1	**0.963 [0.933 ; 0.979]**	**0.944 [0.900 ; 0.968]**	**0.905 [0.835 ; 0.947]**	**0.723 [0.549 ; 0.837]**
ROI-2	**0.940 [0.894 ; 0.966]**	**0.925 [0.867 ; 0.958]**	**0.929 [0.875 ; 0.960]**	**0.316 [0.030 ; 0.555]**
ROI-3	**0.973 [0.951 ; 0.985]**	**0.948 [0.908 ; 0.971]**	**0.955 [0.919 ; 0.975]**	**0.751 [0.590 ; 0.854]**
WoAUC				
ROI-1	**0.979 [0.962 ; 0.989]**	**0.981 [0.965 ; 0.990]**	**0.951 [0.909 ; 0.974]**	**0.827 [0.695 ; 0.905]**
ROI-2	**0.971 [0.948 ; 0.984]**	**0.955 [0.918 ; 0.976]**	**0.943 [0.896 ; 0.969]**	**0.532 [0.254 ; 0.730]**
ROI-3	**0.947 [0.905 ; 0.971]**	**0.951 [0.910 ; 0.973]**	**0.952 [0.911 ; 0.974]**	**0.738 [0.555 ; 0.853]**
AUC				
ROI-1	**0.978 [0.960 ; 0.988]**	**0.984 [0.971 ; 0.991]**	**0.955 [0.917 ; 0.976]**	**0.820 [0.684 ; 0.901]**
ROI-2	**0.969 [0.945 ; 0.983]**	**0.963 [0.932 ; 0.980]**	**0.946 [0.900 ; 0.971]**	**0.472 [0.177 ; 0.690]**
ROI-3	**0.947 [0.905 ; 0.971]**	**0.963 [0.933 ; 0.980]**	**0.954 [0.915 ; 0.976]**	**0.721 [0.530 ; 0.843]**
FT				
ROI-1	0.908 [0.837 ; 0.949]	0.750 [0.581 ; 0.857]	0.710 [0.513 ; 0.836]	0.874 [0.775 ; 0.932]
ROI-2	0.821 [0.696 ; 0.898]	0.733 [0.553 ; 0.848]	0.516 [0.250 ; 0.711]	0.731 [0.536 ; 0.853]
ROI-3	0.924 [0.866 ; 0.958]	0.797 [0.652 ; 0.886]	0.699 [0.496 ; 0.829]	0.696 [0.493 ; 0.828]
WoR				
ROI-1	**0.977 [0.959 ; 0.988]**	**0.972 [0.949 ; 0.985]**	**0.910 [0.836 ; 0.952]**	**0.728 [0.540 ; 0.847]**
ROI-2	**0.947 [0.906 ; 0.971]**	**0.910 [0.839 ; 0.951]**	**0.974 [0.951 ; 0.986]**	**0.254 [0.000 ; 0.534]**
ROI-3	**0.963 [0.934 ; 0.980]**	**0.978 [0.960 ; 0.988]**	**0.979 [0.960 ; 0.989]**	**0.561 [0.304 ; 0.742]**

1

Table 3: ICC values and their 95% confidence interval for evaluation of reproducibility in healthy liver parenchyma.

ICC = intraclass correlation coefficient

Intra = intra-observer reproducibility

Inter = Inter-observer reproducibility

	Day 0		Evolution from day 0 to day 15	
Perfusion parameter	Intra	Inter	Intra	Inter
PE	**0.715 [0.537 ; 0.832]**	**0.960 [0.928 ; 0.978]**	**0.927 [0.872 ; 0.959]**	**0.838 [0.725 ; 0.908]**
WiAUC	**0.503 [0.251 ; 0.692]**	**0.787 [0.644 ; 0.876]**	**0.870 [0.777 ; 0.926]**	**0.619 [0.402 ; 0.771]**
RT	0.682 [0.490 ; 0.812]	0.660 [0.459 ; 0.797]	0.570 [0.336 ; 0.738]	0.694 [0.507 ; 0.819]
mTT	0.247 [0.000 ; 0.500]	0.411 [0.139 ; 0.626]	0.152 [0.000 ; 0.423]	0.447 [0.182 ; 0.652]
TTP	0.748 [0.585 ; 0.853]	0.727 [0.555 ; 0.840]	0.686 [0.495 ; 0.814]	0.732 [0.562 ; 0.843]
WiR	**0.882 [0.795 ; 0.933]**	**0.871 [0.778 ; 0.927]**	**0.955 [0.920 ; 0.975]**	**0.804 [0.671 ; 0.887]**
WoAUC	**0.562 [0.242 ; 0.772]**	**0.860 [0.707 ; 0.937]**	**0.923 [0.810 ; 0.970]**	**0.635 [0.248 ; 0.849]**
AUC	**0.542 [0.215 ; 0.760]**	**0.843 [0.675 ; 0.929]**	**0.924 [0.814 ; 0.971]**	**0.637 [0.251 ; 0.850]**
FT	0.678 [0.412 ; 0.839]	0.562 [0.219 ; 0.782]	0.602 [0.212 ; 0.829]	0.367 [0.000 ; 0.711]
WoR	**0.850 [0.701 ; 0.928]**	**0.890 [0.765 ; 0.950]**	**0.942 [0.855 ; 0.978]**	**0.811 [0.562 ; 0.927]**

Table 4: ICC values and their 95% confidence interval for evaluating reproducibility of normalized perfusion parameters.

ICC = intraclass correlation coefficient

Inter = Inter-observer reproducibility

Intra = intra-observer reproducibility

ROI-1: drawing outlining the lesion in the portal phase DCEUS images

ROI-2: drawing positioned in the hypoenhanced center of the lesion

ROI-3: drawing outlining the lesion based on WiAUC's parametric imaging

	Day 0		Evolution from day 0 to day 15	
Perfusion parameter	Intra	Inter	Intra	Inter
PE				
ROI-1	**0.882 [0.795 ; 0.933]**	**0.897 [0.822 ; 0.942]**	**0.477 [0.218 ; 0.674]**	**0.684 [0.492 ; 0.812]**
ROI-2	**0.929 [0.874 ; 0.960]**	**0.879 [0.792 ; 0.932]**	**0.760 [0.604 ; 0.860]**	**0.721 [0.547 ; 0.836]**
ROI-3	**0.905 [0.834 ; 0.946]**	**0.868 [0.773 ; 0.925]**	**0.670 [0.472 ; 0.803]**	**0.688 [0.498 ; 0.815]**
WiAUC				
ROI-1	**0.700 [0.516 ; 0.823]**	**0.684 [0.493 ; 0.813]**	**0.447 [0.181 ; 0.652]**	**0.387 [0.110 ; 0.608]**
ROI-2	**0.836 [0.722 ; 0.906]**	**0.766 [0.613 ; 0.864]**	**0.715 [0.537 ; 0.832]**	**0.647 [0.440 ; 0.789]**
ROI-3	**0.705 [0.522 ; 0.826]**	**0.677 [0.483 ; 0.808]**	**0.647 [0.440 ; 0.789]**	**0.547 [0.307 ; 0.722]**
RT				
ROI-1	0.515 [0.266 ; 0.700]	0.425 [0.156 ; 0.637]	0.451 [0.187 ; 0.655]	0.496 [0.242 ; 0.687]
ROI-2	0.456 [0.193 ; 0.659]	0.416 [0.145 ; 0.630]	0.564 [0.328 ; 0.733]	0.574 [0.341 ; 0.740]
ROI-3	0.522 [0.274 ; 0.705]	0.452 [0.188 ; 0.656]	0.446 [0.181 ; 0.652]	0.480 [0.222 ; 0.676]
mTT				
ROI-1	0.431 [0.163 ; 0.641]	0.201 [0.000 ; 0.463]	0.071 [0.000 ; 0.353]	0.715 [0.537 ; 0.832]
ROI-2	0.288 [0.000 ; 0.533]	0.282 [0.000 ; 0.528]	0.006 [0.000 ; 0.295]	0.618 [0.401 ; 0.770]
ROI-3	0.471 [0.211 ; 0.669]	0.283 [0.000 ; 0.529]	0.124 [0.000 ; 0.399]	0.730 [0.560 ; 0.842]
TTP				

ROI-1	0.594 [0.368 ; 0.754]	0.579 [0.349 ; 0.744]	0.648 [0.442 ; 0.789]	0.605 [0.383 ; 0.761]
ROI-2	0.499 [0.246 ; 0.689]	0.555 [0.317 ; 0.728]	0.684 [0.493 ; 0.813]	0.663 [0.463 ; 0.799]
ROI-3	0.605 [0.384 ; 0.761]	0.610 [0.391 ; 0.765]	0.652 [0.448 ; 0.792]	0.611 [0.391 ; 0.765]
WiR				
ROI-1	**0.877 [0.787 ; 0.930]**	**0.869 [0.775 ; 0.926]**	**0.492 [0.238 ; 0.684]**	**0.776 [0.627 ; 0.870]**
ROI-2	**0.884 [0.799 ; 0.934]**	**0.839 [0.726 ; 0.908]**	**0.800 [0.664 ; 0.884]**	**0.768 [0.616 ; 0.865]**
ROI-3	**0.891 [0.810 ; 0.938]**	**0.840 [0.727 ; 0.908]**	**0.614 [0.396 ; 0.767]**	**0.746 [0.583 ; 0.852]**
WoAUC				
ROI-1	**0.626 [0.327 ; 0.812]**	**0.774 [0.543 ; 0.897]**	**0.581 [0.166 ; 0.823]**	**0.521 [0.082 ; 0.794]**
ROI-2	**0.797 [0.602 ; 0.903]**	**0.812 [0.598 ; 0.919]**	**0.663 [0.307 ; 0.858]**	**0.537 [0.069 ; 0.815]**
ROI-3	**0.688 [0.421 ; 0.846]**	**0.737 [0.479 ; 0.879]**	**0.525 [0.087 ; 0.796]**	**0.393 [0.000 ; 0.726]**
AUC				
ROI-1	**0.633 [0.337 ; 0.816]**	**0.785 [0.563 ; 0.902]**	**0.539 [0.106 ; 0.803]**	**0.571 [0.151 ; 0.818]**
ROI-2	**0.804 [0.613 ; 0.906]**	**0.814 [0.602 ; 0.920]**	**0.692 [0.355 ; 0.872]**	**0.616 [0.185 ; 0.851]**
ROI-3	**0.691 [0.426 ; 0.848]**	**0.738 [0.482 ; 0.879]**	**0.503 [0.057 ; 0.784]**	**0.424 [0.000 ; 0.743]**
FT				
ROI-1	0.495 [0.146 ; 0.736]	0.320 [0.000 ; 0.640]	0.622 [0.228 ; 0.843]	0.397 [0.000 ; 0.727]
ROI-2	0.376 [0.000 ; 0.660]	0.221 [0.000 ; 0.586]	0.390 [0.000 ; 0.716]	0.357 [0.000 ; 0.723]
ROI-3	0.465 [0.108 ; 0.718]	0.321 [0.000 ; 0.640]	0.431 [0.000 ; 0.747]	0.311 [0.000 ; 0.678]
WoR				
ROI-1	**0.779 [0.570 ; 0.894]**	**0.840 [0.663 ; 0.928]**	**0.746 [0.437 ; 0.899]**	**0.478 [0.024 ; 0.771]**
ROI-2	**0.578 [0.258 ; 0.785]**	**0.811 [0.596 ; 0.918]**	**0.916 [0.794 ; 0.967]**	**0.563 [0.105 ; 0.827]**
ROI-3	**0.809 [0.622 ; 0.909]**	**0.825 [0.635 ; 0.921]**	**0.832 [0.604 ; 0.935]**	**0.375 [0.000 ; 0.715]**

1

Table 5: Quality of WiAUC's parametric imaging, area of the regions of interest (ROI) and quality of the mathematical fit. Quantitative variables are described using quartiles, and qualitative variables are described using numbers and frequencies.

ROI-1: ROI outlining the lesion in the portal phase DCEUS images

ROI-2: ROI positioned in the hypoenhanced center of the lesion

ROI-3: ROI outlining the lesion based on WiAUC's parametric imaging

D0: evaluation at day 0

D15: evaluation at day 15

Variable	Values	
Quality (Q) of WiAUC's parametric imaging[1]	Q < 10%: 13 (4.8)	
	10% ≤ Q < 50%: 27 (10.0)	
	50% ≤ Q < 75%: 72 (26.7)	
	Q ≥ 75%: 158 (58.5)	
Area of the ROIs (cm²)	D0	ROI-1: 6.2 [3.5 ; 12.7] ROI-2: 3.3 [1.4 ; 6.2] ROI-3: 7.1 [4.0 ; 13.5]
	D15	ROI-1: 5.2 [2.9 ; 11.1] ROI-2: 2.6 [1.2 ; 5.3] ROI-3: 6.1 [3.7 ; 10.9]
Quality of fit (%)	D0	ROI-1: 92.3 [80.6 ; 96.7] ROI-2: 89.8 [74.8 ; 97.0] ROI-3: 93.1 [87.6 ; 96.4]
	D15	ROI-1: 89.4 [82.7 ; 95.7] ROI-2: 86.9 [76.8 ; 94.7]

		ROI-3: 92.7 [85.4 ; 95.3]

[1] total = 270 (3*45 at day 0 + 3*45 for the evolution between day 15 and day 0)

Acknowledgments: Authors thank physicians and radiologists of all centers (Reims, Besançon, Nantes, Bordeaux, Angers, Paris, Poitiers and Rennes) for their contribution in patients' inclusions and ultrasound exams. Authors thank François Tranquart for his contributive advices.

REFERENCES:

Atri M, Hudson JM, Sinaei M, Williams R, Milot L, Moshonov H, Burns PN, Bjarnason GA. Impact of Acquisition Method and Region of Interest Placement on Inter-observer Agreement and Measurement of Tumor Response to Targeted Therapy Using Dynamic Contrast-Enhanced Ultrasound. Ultrasound Med Biol 2016;42:763–768.

Choi H, Charnsangavej C, Faria SC, Macapinlac HA, Burgess MA, Patel SR, Chen LL, Podoloff DA, Benjamin RS. Correlation of computed tomography and positron emission tomography in patients with metastatic gastrointestinal stromal tumor treated at a single institution with imatinib mesylate: proposal of new computed tomography response criteria. J Clin Oncol Off J Am Soc Clin Oncol 2007;25:1753–1759.

Chun YS, Vauthey J-N, Boonsirikamchai P, Maru DM, Kopetz S, Palavecino M, Curley SA, Abdalla EK, Kaur H, Charnsangavej C, Loyer EM. Association of computed tomography morphologic criteria with pathologic response and survival in patients treated with bevacizumab for colorectal liver metastases. JAMA 2009;302:2338–2344.

Claudon M, Dietrich CF, Choi BI, Cosgrove DO, Kudo M, Nolsøe CP, Piscaglia F, Wilson SR, Barr RG, Chammas MC, Chaubal NG, Chen M-H, Clevert DA, Correas JM, Ding H, Forsberg F, Fowlkes JB, Gibson RN, Goldberg BB, Lassau N, Leen ELS, Mattrey RF, Moriyasu F, Solbiati L, Weskott H-P, Xu H-X, World Federation for Ultrasound in Medicine, European Federation of Societies for Ultrasound. Guidelines and good clinical practice recommendations for Contrast Enhanced Ultrasound (CEUS) in the liver - update 2012: A WFUMB-EFSUMB initiative in cooperation with representatives of AFSUMB, AIUM, ASUM, FLAUS and ICUS. Ultrasound Med Biol 2013;39:187–210.

Coenegrachts K, Bols A, Haspeslagh M, Rigauts H. Prediction and monitoring of treatment effect using T1-weighted dynamic contrast-enhanced magnetic resonance imaging in colorectal liver metastases: potential of whole tumour ROI and selective ROI analysis. Eur J Radiol 2012;81:3870–3876.

De Bruyne S, Van Damme N, Smeets P, Ferdinande L, Ceelen W, Mertens J, Van de Wiele C, Troisi R, Libbrecht L, Laurent S, Geboes K, Peeters M. Value of DCE-MRI and FDG-PET/CT in the prediction of response to preoperative chemotherapy with bevacizumab for colorectal liver metastases. Br J Cancer 2012;106:1926–1933.

Desar IME, van Herpen CML, van Laarhoven HWM, Barentsz JO, Oyen WJG, van der Graaf WTA. Beyond RECIST: molecular and functional imaging techniques for evaluation of response to targeted therapy. Cancer Treat Rev 2009;35:309–321.

Dietrich CF, Averkiou M, Nielsen MB, Barr RG, Burns PN, Calliada F, Cantisani V, Choi B, Chammas MC, Clevert D-A, Claudon M, Correas J-M, Cui X-W, Cosgrove D, D'Onofrio M, Dong Y, Eisenbrey J, Fontanilla T, Gilja OH, Ignee A, Jenssen C, Kono Y, Kudo M, Lassau N, Lyshchik A, Franca Meloni M, Moriyasu F, Nolsøe C, Piscaglia F, Radzina M, Saftoiu A, Sidhu PS, Sporea I, Schreiber-Dietrich D, Sirlin CB,

Stanczak M, Weskott H-P, Wilson SR, Willmann JK, Kim TK, Jang H-J, Vezeridis A, Westerway S. How to perform Contrast-Enhanced Ultrasound (CEUS). Ultrasound Int Open 2018;4:E2–E15.

Dietrich CF, Averkiou MA, Correas J-M, Lassau N, Leen E, Piscaglia F. An EFSUMB introduction into Dynamic Contrast-Enhanced Ultrasound (DCE-US) for quantification of tumour perfusion. Ultraschall Med Stuttg Ger 1980 2012;33:344–351.

Eisenhauer EA, Therasse P, Bogaerts J, Schwartz LH, Sargent D, Ford R, Dancey J, Arbuck S, Gwyther S, Mooney M, Rubinstein L, Shankar L, Dodd L, Kaplan R, Lacombe D, Verweij J. New response evaluation criteria in solid tumours: revised RECIST guideline (version 1.1). Eur J Cancer Oxf Engl 1990 2009;45:228–247.

Gauthier M, Leguerney I, Thalmensi J, Chebil M, Parisot S, Peronneau P, Roche A, Lassau N. Estimation of intra-operator variability in perfusion parameter measurements using DCE-US. World J Radiol 2011;3:70–81.

Goh V, Halligan S, Gharpuray A, Wellsted D, Sundin J, Bartram CI. Quantitative assessment of colorectal cancer tumor vascular parameters by using perfusion CT: influence of tumor region of interest. Radiology 2008;247:726–732.

Goh V, Padhani AR, Rasheed S. Functional imaging of colorectal cancer angiogenesis. Lancet Oncol 2007;8:245–255.

Grothey A, Allegra C. Antiangiogenesis therapy in the treatment of metastatic colorectal cancer. Ther Adv Med Oncol 2012;4:301–319.

Hurwitz H, Fehrenbacher L, Novotny W, Cartwright T, Hainsworth J, Heim W, Berlin J, Baron A, Griffing S, Holmgren E, Ferrara N, Fyfe G, Rogers B, Ross R, Kabbinavar F. Bevacizumab plus irinotecan, fluorouracil, and leucovorin for metastatic colorectal cancer. N Engl J Med 2004;350:2335–2342.

Konerding MA, Fait E, Gaumann A. 3D microvascular architecture of pre-cancerous lesions and invasive carcinomas of the colon. Br J Cancer 2001;84:1354–1362.

Krajewski KM, Guo M, Van den Abbeele AD, Yap J, Ramaiya N, Jagannathan J, Heng DYC, Atkins MB, McDermott DF, Schutz FAB, Pedrosa I, Choueiri TK. Comparison of four early posttherapy imaging changes (EPTIC; RECIST 1.0, tumor shrinkage, computed tomography tumor density, Choi criteria) in assessing outcome to vascular endothelial growth factor-targeted therapy in patients with advanced renal cell carcinoma. Eur Urol 2011;59:856–862.

Lassau N, Bonastre J, Kind M, Vilgrain V, Lacroix J, Cuinet M, Taieb S, Aziza R, Sarran A, Labbe-Devilliers C, Gallix B, Lucidarme O, Ptak Y, Rocher L, Caquot L-M, Chagnon S, Marion D, Luciani A, Feutray S, Uzan-Augui J, Coiffier B, Benastou B, Koscielny S. Validation of dynamic contrast-enhanced ultrasound in predicting outcomes of antiangiogenic therapy for solid tumors: the French multicenter support for innovative and expensive techniques study. Invest Radiol 2014;49:794–800.

Lassau N, Coiffier B, Kind M, Vilgrain V, Lacroix J, Cuinet M, Taieb S, Aziza R, Sarran A, Labbe-Devilliers C, Gallix B, Lucidarme O, Ptak Y, Rocher L, Caquot LM, Chagnon S, Marion D, Luciani A, Feutray S, Uzan-Augui J, Benatsou B, Bonastre J, Koscielny S. Selection of an early biomarker for vascular normalization using dynamic contrast-enhanced ultrasonography to predict outcomes of metastatic patients treated with bevacizumab. Ann Oncol Off J Eur Soc Med Oncol 2016;27:1922–1928.

Lassau N, Koscielny S, Albiges L, Chami L, Benatsou B, Chebil M, Roche A, Escudier BJ. Metastatic renal cell carcinoma treated with sunitinib: early evaluation of treatment response using dynamic contrast-enhanced ultrasonography. Clin Cancer Res Off J Am Assoc Cancer Res 2010;16:1216–1225.

Lassau N, Koscielny S, Chami L, Chebil M, Benatsou B, Roche A, Ducreux M, Malka D, Boige V. Advanced hepatocellular carcinoma: early evaluation of response to bevacizumab therapy at dynamic contrast-enhanced US with quantification--preliminary results. Radiology 2011;258:291–300.

Lassau N, Lamuraglia M, Chami L, Leclère J, Bonvalot S, Terrier P, Roche A, Le Cesne A. Gastrointestinal stromal tumors treated with imatinib: monitoring response with contrast-enhanced sonography. AJR Am J Roentgenol 2006;187:1267–1273.

Lyshchik A, Kono Y, Dietrich CF, Jang H-J, Kim TK, Piscaglia F, Vezeridis A, Willmann JK, Wilson SR. CONTRAST-ENHANCED ULTRASOUND OF THE LIVER: TECHNICAL AND LEXICON RECOMMENDATIONS FROM THE ACR CEUS LI-RADS WORKING GROUP. Abdom Radiol N Y 2018;43:861–879.

Morgan B, Thomas AL, Drevs J, Hennig J, Buchert M, Jivan A, Horsfield MA, Mross K, Ball HA, Lee L, Mietlowski W, Fuxuis S, Unger C, O'Byrne K, Henry A, Cherryman GR, Laurent D, Dugan M, Marmé D, Steward WP. Dynamic contrast-enhanced magnetic resonance imaging as a biomarker for the pharmacological response of PTK787/ZK 222584, an inhibitor of the vascular endothelial growth factor receptor tyrosine kinases, in patients with advanced colorectal cancer and liver metastases: results from two phase I studies. J Clin Oncol Off J Am Soc Clin Oncol 2003;21:3955–3964.

Payen T, Guibal A, Lamuraglia M, Lucidarme O, Arditi M, Guillou DL, Bridal SL. Choice and normalization of contrast ultrasound parameters for detection of anti-angiogenic response. 2011 IEEE Int Ultrason Symp 2011. pp. 1486–1489.

R Development Core Team. R: A Language And Environment for Statistical Computing. Vienna, Austria: R Foundation for Statistical Computing, 2016. Available from: https://www.R-project.org

Schirin-Sokhan R, Winograd R, Roderburg C, Bubenzer J, do Ó NC, Guggenberger D, Hecker H, Trautwein C, Tischendorf JJW. Response evaluation of chemotherapy in metastatic colorectal cancer by contrast enhanced ultrasound. World J Gastroenterol 2012;18:541–545.

Shindoh J, Loyer EM, Kopetz S, Boonsirikamchai P, Maru DM, Chun YS, Zimmitti G, Curley SA, Charnsangavej C, Aloia TA, Vauthey J-N. Optimal morphologic response to preoperative chemotherapy: an alternate outcome end point before resection of hepatic colorectal metastases. J Clin Oncol Off J Am Soc Clin Oncol 2012;30:4566–4572.

Tranquart F, Dujardin P-A, Bouché O, Marcus C, Borg C, Manzoni P, Douillard J-Y, Labbe-Devilliers C, Terrebonne E, Smith D, Trillaud H, Capitain O, Aubé C, Spano J-P, Lucidarme O, Ferru A, Tasu J-P, Manfredi S, Bleuzen A, Léger J, Lecomte T. Value of Contrast-Enhanced Ultrasound Quantification Criteria for Identifying Patients not Responding to Bevacizumab-Based Therapy for Colorectal Liver Metastases. Ultraschall Med Stuttg Ger 1980 2017;

Tranquart F, Mercier L, Frinking P, Gaud E, Arditi M. Perfusion quantification in contrast-enhanced ultrasound (CEUS)--ready for research projects and routine clinical use. Ultraschall Med Stuttg Ger 1980 2012;33 Suppl 1:S31-38.

Williams R, Hudson JM, Lloyd BA, Sureshkumar AR, Lueck G, Milot L, Atri M, Bjarnason GA, Burns PN. Dynamic microbubble contrast-enhanced US to measure tumor response to targeted therapy: a proposed clinical protocol with results from renal cell carcinoma patients receiving antiangiogenic therapy. Radiology 2011;260:581–590.

Wu Z, Yang X, Chen L, Wang Z, Shi Y, Mao H, Dai G, Yu X. Anti-angiogenic therapy with contrast-enhanced ultrasound in colorectal cancer patients with liver metastasis. Medicine (Baltimore) 2017;96:e6731.

Figure 1: Drawing of Regions of Interest (ROI) in liver metastasis of colorectal cancer for quantification of perfusion. (a) Reference ROI (green) is drawn in healthy liver parenchyma and ROI-1 (yellow) delineates the tumor based on portal phase DCEUS image. (b) ROI-2 (purple) is drawn in the central part of the lesion and ROI-3 (white) delineates the tumor based on WiAUC's parametric imaging in (c).

Figure 2: Visual representation of perfusion parameters reproducibility. All data have been extracted from tables 2 to 4. A green cell represents ICC $\geq$ 0.9. A blue cell represents 0.8 $\leq$ ICC < 0.9. A red cell represents 0.7 $\leq$ ICC < 0.8. Other cells represent ICC < 0.7.

D0: evaluation at day 0

D15-D0: evaluation of the evolution between day 15 and day 0.

Inter = inter-observer reproducibility

Intra = intra-observer reproducibility

ICC = intraclass correlation coefficient

Figure 3: Inclusion of hyperenhanced rim in parametric ROIs. (a) On arterial phase, an hyperenhanced rim is clearly visible (arrows). (b) WiAUC's parametric imaging allows good delineation of the tumor (ROI-3, white) and hyperenhanced rim is often seen as a peripheral rim with different WiAUC from the rest of the lesion. (c) ROI-1 (yellow) and ROI-3 (white) are drawn with their respective rules. (d) Back to arterial phase, ROI-1 (yellow) does not include the entire hyperenhanced rim while ROI-3 (white) does.


38
18
a
b
c

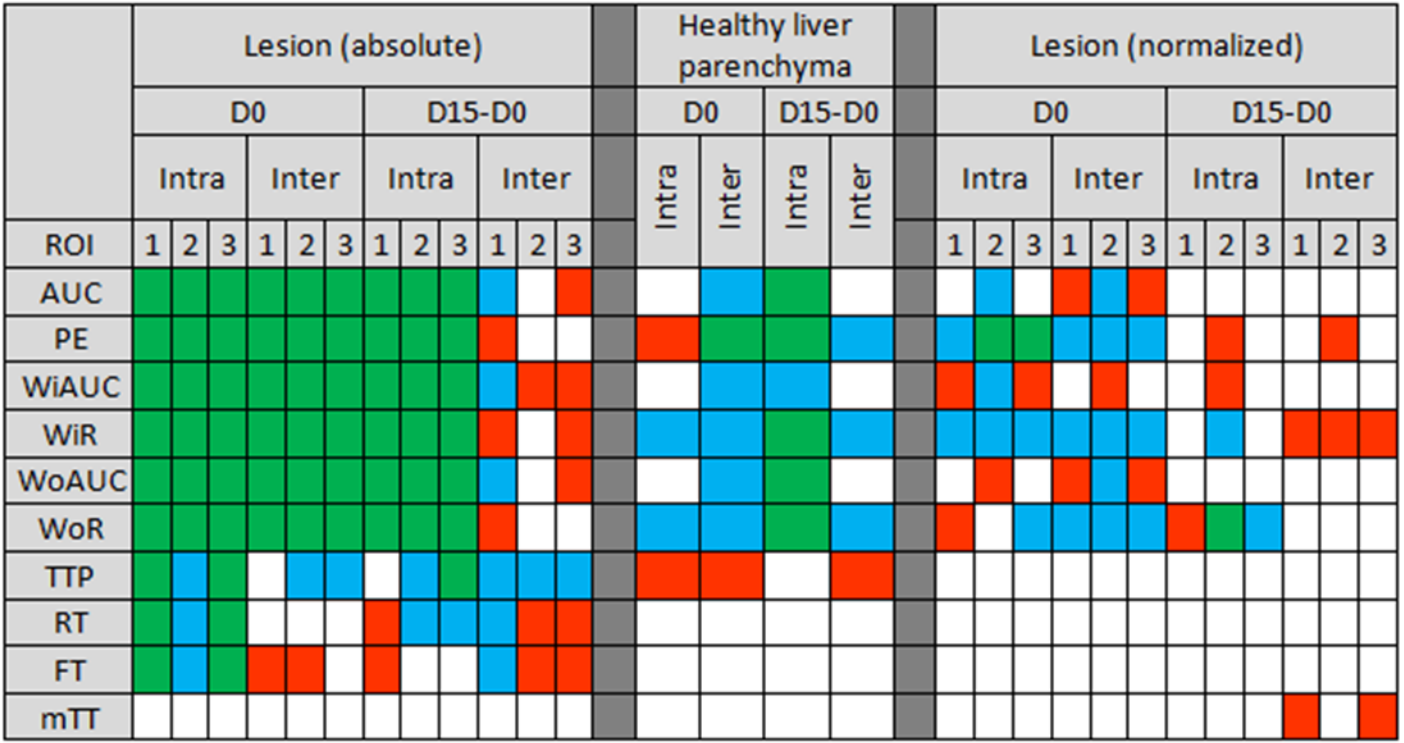
Lesion (absolute)
Healthy liver parenchyma
Lesion (normalized)
D0
D15-D0
Intra
Inter
ROI
1 2 3
AUC
PE
WiAUC
WiR
WoAUC
WoR
TTP
RT
FT
mTT

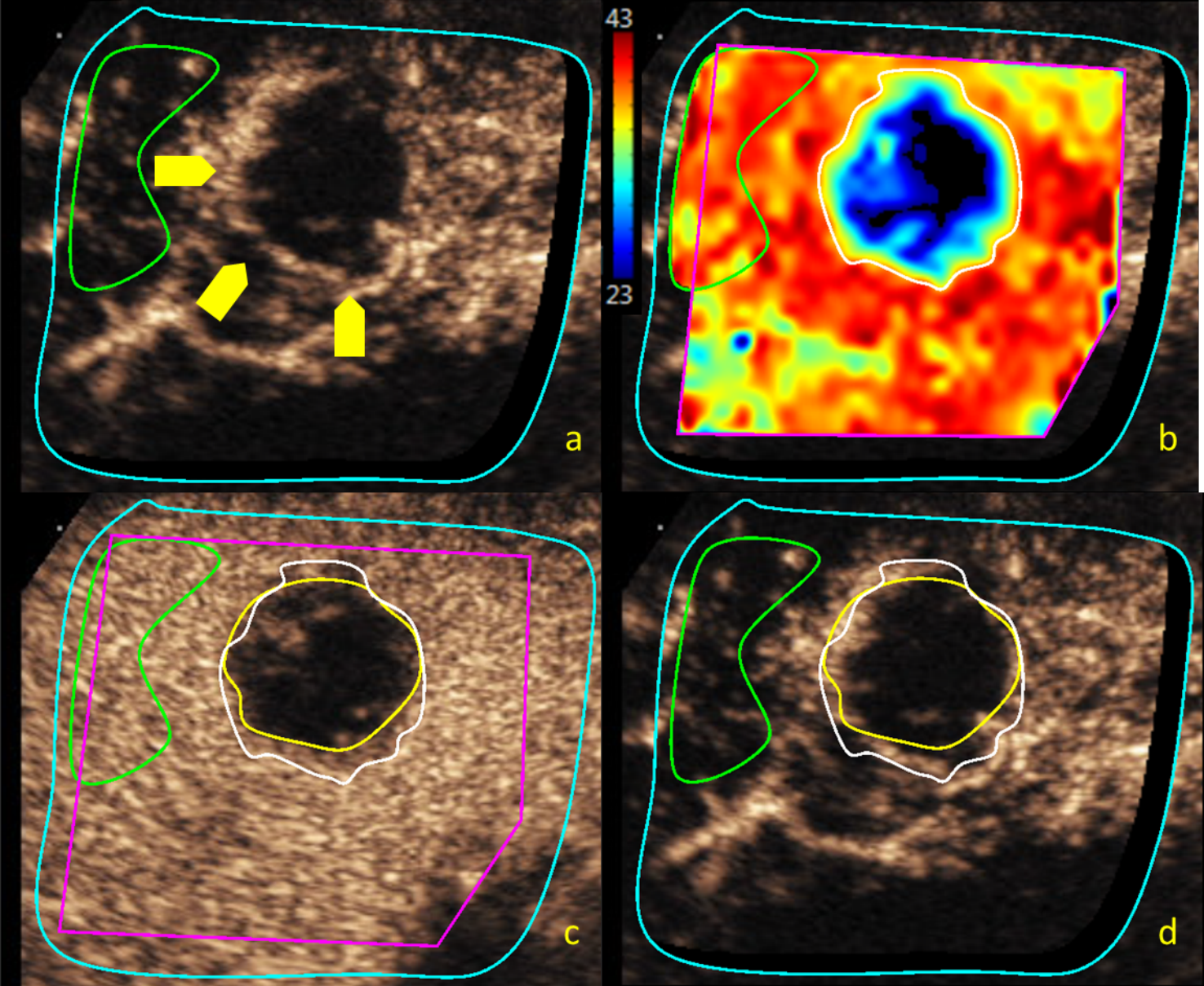
43
23
a
b
c
d